International Journal of Scientific Research in Science and Technology
Print ISSN: 2395-6011 | Online ISSN: 2395-602X (www.ijsrst.com)
doi : https://doi.org/10.32628/IJSRST229381

Spatio-temporal variability of Turbidity over Ukai Reservoir, by using RS2/R2A LISS III Satellite datasets

V. Pompapathi*[1], Ashwin Gujrati[2], Shard Chander[3], H. A. Solanki[4]

[*1,] Land Hydrology Division, GHCAG/EPSA, Space Applications Centre, ISRO, Ahmedabad, India
Department of Environmental Science, Gujarat University, Ahmedabad, India

[2] Land Hydrology Division, GHCAG/EPSA, Space Applications Centre, ISRO, Ahmedabad, India

[3] Land Hydrology Division, GHCAG/EPSA, Space Applications Centre, ISRO, Ahmedabad, India

[4]Department of Environmental Science, Gujarat University, Ahmedabad, India

Article Info
Volume 9, Issue 3
Page Number : 377-386

Publication Issue
May-June-2022

Article History
Accepted : 01 June 2022
Published : 05 June 2022

ABSTRACT

Turbidity is an optical determination of water clarity. It is one of the most important optically active water parameter to assess the water quality through the remote sensing observations. Turbidity measurements come from suspension of sediment such as silt or clay, inorganic materials, or organic matter such as algae, plankton and decaying material. Turbidity and total suspended matter often overlap each other. However, it is not a direct measurement of the total suspended materials in water. Instead, as a measure of relative clarity, turbidity is often used to indicate changes in the total suspended solids concentration in water without providing an exact measurement of solids. Through remote sensing we can monitor the turbidity in large water bodies, rives, coastal areas etc. An algorithm has been developed to estimate the turbidity (in NTU: Nephelometric Turbidity Unit) over inland waters (Ukai reservoir) using empirical relationship between normalized Green and Red bands (NDTI : Normalized Difference Turbidity Index) of Resourcesat-2 and Resourcsat-2A Linear Imaging Self Scanning-III (RS2 and R2A LISS-III) dataset. Derived algorithm shows a strong coefficient of determination (R2 = 0.97) with the in-situ turbidity measurements. The field measurements were carried out over Ukai reservoir on 27-28th March 2018, where synchronous in situ water leaving reflectance and turbidity were measured. Model was derived between in situ measured turbidity and NDTI derived from spectral reflectance of band 2 (Green) and band 3 (Red) of RS2 and R2A LISS-III. The model was applied to derive the turbidity maps of Ukai reservoir for pre-monsoon (March, April and May months) season during the period 2012 to 2018. Overall turbidity ranges from 1.47-20 NTU during the field data collection of pre-monsoon season and overall scene derived turbidity ranges are between 2 – 33 NTU. The highest observed turbidity value was more than fourteen times

greater than the lowest value that shows the natural variability within the reservoir for the same season. Remotely sensed data sets can increase the abilities of water resources researchers and decision making persons to monitor waterbodies more effectively and frequently.

Keywords: Turbidity, Ukai Reservoir, Resourcesat2, Resourcesat2A, Relative Spectral Response (RSR).

I. INTRODUCTION

Turbidity is an optical property of water, which scatters and absorbs the light rather than transmit it in straight lines. It is a major influenceing parameter of the aquatic system, is determined by the light absorption and scattering processes that take place within the water column [6]. Turbidity and total suspended matters (TSM) are considered as important water quality variables in many environmental studies due to their linkage with incoming sunlight that in turn affects photosynthesis for growth of algae and plankton [12]. It reduces light penetration into the water and which affect the entire aquatic ecosystem [11]. Observations on TSM can be used in various numerical schemes to help characterize the trophic state of an aquatic ecosystem [7] [30]. Knowing precise spatial and temporal turbidity information of aquatic ecosystem is necessary to both protect the lake ecosystem and maintain the water quality management [14] [8] [26]. Satellite and airborne remote sensing data sets has proven its usefulness in mapping some of the most importrant optically active water quality parameters such as turbidity, TSM, and chlorophyll-a [5] [15] [16] [25].

Remote sensing techniques has been widely used to estimate and map the turbidity and concentrations of suspended particles [3]. The advantage of remote sensing is, it can provide a synoptical view of the complete water body due to it's continuous, spatial and temporal coverage of large areas coverage. Satellite have global coverage and also includes the in-accessible locations/harsh enviornmet where ground data is not available. Furthermore it provides long term and historical water quality monitoring possible with satellite data sets.

Improvements in remote sensing techniques made possible to regular monitoring the optically active components like turbidity and chlorophyll-a of inland water bodies, like lakes and reservoirs [19]. Imaging spectroscopy is well esatablished method to assess water quality but there are limited airborne and space borne measurements with required spatial resoluton avaialble over inland water bodies especially over rives. Multi spectral sensors onboard Landsat and SPOT satellite series have been used to assess water quality related paramentes over lakes, reservoirs and rivers using different band ratios and single band algorithm. In recent decads, a number of studies have demonstrated that suspended sediments distribution in open sea and inland waters can be mapped from different types of satellite remote sensing data, such as Landsat satellite series, Moderate Imaging Spectroradiometer (MODIS), and Medium Resolution Imaging Spectrometer (MERIS) [29] [18] [21].

Turbidity values generally correlates well with reflectance at satellite bands located in the red part of the spectrum for low to moderate turbidity values. Landsat band 3 (630-690 nm) has been used to map turbidity in Guadalquivir River (Spain) for a turbidity range 1.5 – 8 NTU [2]. A good correlation was observed between LISS-I red band (620-680 nm) and

turbidity in the range of 15-45 NTU in the Tawa reservoir in India [10]. [13] used SPOT-HRV2 red band (610-680 nm) to map relatively low levels of turbidity, ranged from 3 to 15 NTU, in the Tuttel Creek reservoir in Kansas, USA. [23] developed a regional alogortm for MODIS-Aqua 250 m red band to map turbidity in the Adour river plume (Bay of Biacay, France), where field turbidity values varied between 0.5 and 70 NTU. A multiple linear regression analysis using Landsat red band (630-690 nm) and near infrared (750-900 nm) bands was used to predict turbidity in a glacial lake in Alaska where highly scatter rock flower (Sediment oriented from glacial rock weathering) dominates the perticulate fraction.

No global standardized turbidity derived algorithm exists in scientific community because of the high level of variation in particle size, density and other optical complexities of different water bodies [4]. As per our knowledge, this is the first attempt to develop algorithm for assessment of turbidity over Ukai reservoir using Indian Remote Sensing multi spectral sensors: Resourcesat 2 and 2A Linear Imaging Self Scanning-III (RS2 and R2A-LISS-III). The algorithm was used for estimation of spatial and temporal variability of turbidity during premonsoon season of Ukai reservoir for the last 7 years (2012-2018).

II. STUDY AREA AND MATERIALS

A. Study area

Ukai Reservoir constructed on the river Tapi, is the second largest reservoir in Gujarat, India after Sardar sarovar. The total area of the reservoir is 494.01km^2. The river has a Total length of 720 km out of which 208 km lies in the Madhya Pradesh, 323 km in the Maharastra and 189 km in Gujarat. It ultimately meets the Arabian Sea approximately 19.2 km west of surat in Gujarat. Ukai Reservoir catchment area is 62225 km^2, mean and maximum annual rainfall in the watershed 785 and 1191 mm respectively.

The The reservoir is meant for power production, irrigation and flood control. The reservoir also provides water for domestic and industrial use in Surat city and surrounding areas. Average annual rainfall in the catchment is about 900 mm and mostly concentrated in monsoon moths (July and August). In this study based on the observe variation in turbidity and the bathymetry, the resevoir area is divided (Figure 1) [24] into three parts, i.e. Down (A), Middle (B) and Up streams (C) for analyzing the variation of water quality parameters.

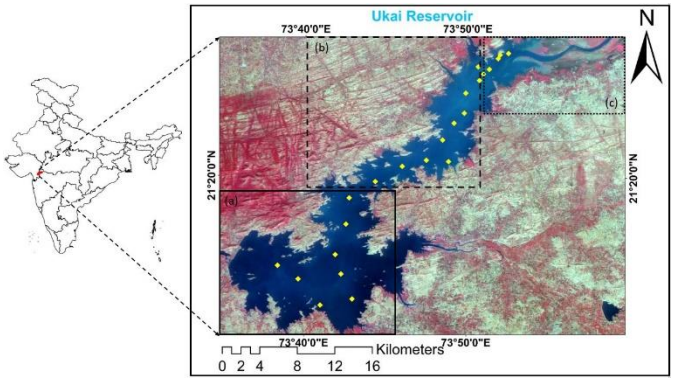

Figure 1. Study area map of Ukai reservoir in India, with Down (a), Middle (b) and Up Streams (c) and insitu sampling points

B. Satellite data acquisition

Three types of data set acquired for the analysis, includes (1) *in-situ* Remote Sensing Reflectance (Rrs), (2) *in-situ* turbidity measurements and (3) RS2 and R2A LISS-III (Path/Row: 94/57) satellite radaince data for the duartion 2012-2018 (Table 1).

Table 1. RS2 and R2A LISS III satellite data used in the Study.

	Acquisition date (YYYY/MM/DD)	Satellite-Sensor
1	2012-03-02	RS2 LISS-III
2	2012-03-26	RS2 LISS-III
3	2013-03-21	RS2 LISS-III
4	2013-04-14	RS2 LISS-III
5	2013-05-08	RS2 LISS-III
6	2014-03-16	RS2 LISS-III
7	2014-04-09	RS2 LISS-III
8	2015-03-11	RS2 LISS-III
9	2015-04-28	RS2 LISS-III

10	2015-05-22	RS2 LISS-III
11	2016-03-05	RS2 LISS-III
12	2016-04-22	RS2 LISS-III
13	2016-05-16	RS2 LISS-III
14	2017-03-12	R2A LISS-III
15	2017-04-05	R2A LISS-III
16	2017-05-11	RS2 LISS-III
17	2018-03-31*	R2A LISS-III
18	2018-04-24	R2A LISS-III
19	2018-05-06	RS2 LISS-III

*The asterisked file (2018-03-31) was the IRS-2A LISS-III image, which was the nearest pass date to field work dates

RS2 and R2A LISS-III Level-1 geometric terrain corrected (GTD) data was procuered form the National Remote Sensing Center site (NRSC, http://nrsc.gov.in). LISS-III dataset is 10-bit quantized and has spatial resolution of 24 m with swath of 141 km. More details about the sensor are provides in the Table 2. This study mainly concentrates on the pre-monsoon season, i.e. March to May, in which total 19 cloud free images were analyzed during the period of this study.

Table 2. RS2 and R2A LISS-III sensors characteristcs

Sensor	Green Band	Red Band	NIR Band	SWIR Band
RS2/R2A-LISS-III (Wave length) (mm)	0.52-0.59	0.62-0.68	0.77-0.86	1.55-1.70
RS2/R2A-LISS-III (Exoatmospheric spectral irradiance Eo (W m^{-2} μm^{-1}))	1850.05	1588.86	1106.72	241.80

Source: [22]

C. Field data collection

The field measurements were carried out over Ukai reservoir on 27-28th March 2018, where *in-situ* water leaving reflectance and turbidity was measured. There were total 23 sampling sites ranging from turbid to clear water. At every site, the turbidity was measured with the Wetlabs Turbidity meter (NTU-B) and the co-ordinates were marked using a Global Positioning System (GPS). An ASD FieldSpec spectroradiometer was used to measure spectral reflectance that has spectral range of 350-2500 nm. In accordance with the Ocean Optics protocols [1] [20], the above-water measurement method was used to measure the radiance spectra of the white reference panel, water, and sky respectively We acquired in situ hyperspectral reflectance data using an Analytical Spectral Devices (ASD)

spectroradiometer at 1.5 m above the water surface. The instrument uses three separate detectors spanning the visible, near-infrared (VNIR), and shortwave infrared (SWIR1 and SWIR2) with a spectral sampling interval of 1.4 nm for the VNIR detector and 1.0 nm for the SWIR detectors. The spectral measurement is resampled and reported for every 1 nm. The majority of in situ remote sensing samples were acquired from 09:30 to 11:00 am and from 2:00 to 4:30 pm local time on 27-28th March 2018. Above water radiometry measurement and data analysis was done performed as per IOCCG protocols for *in situ* optical radiometry [32]. The measurement equation for the water-leaving radiance L_W is given by

$$L_W = L_T - \rho L_I$$

where ρ is the sea surface reflectance factor with the wind speed, L_T is total radiance from the water and L_I is Sky radiance.

The remote sensing reflectance was derived based on the below equation [27].

$$R_{rs}(\lambda) = (L_t - r^*L_{sky})/(L_p^*\pi/\rho_p) \quad (1)$$

where $R_{rs}(\lambda)$ is remote sensing reflectance, L_t is the measured total radiance of the water surface, r is skylight reflectance at the air-water surface; L_{sky} is the measured radiance from sky; L_p is the measured of

the reference panel; and ρ_p is reflectance of the diffuse panel [31].

III. METHODOLOGY

The field-collected *in situ* spectra were converted into simulated bandpass RS2 and R2A LISS-III sensor reflectance using Relative Spectral Response (RSR) function for each channel. To aggregate the reflectance following equation is used.

$$R_b = \frac{\sum_{\lambda_m}^{\lambda_n} RSR_b(\lambda) * R(\lambda) d\lambda}{\sum_{\lambda_m}^{\lambda_n} RSR_b(\lambda)} \quad (2)$$

Where R_b denotes simulated aggregate reflectance at band b. $RSR_b(\lambda)$ represent Relative Spectral Response function of band b within a range from λ_m to λ_n channels and $R(\lambda)$ is *in situ* reflectance spectra.

The parametric algorithm based on the combination of bands was tested for estimating the best correlation between water turbidity and simulated RS2 and R2A LISS-III derived reflectance (R_b). Modified Normalized Difference Water Index (MNDWI) [28] was used to mask out pixels other than water in images. Several linear and non-linear models were explored out over bands and band combination using least square fitting technique to find the best coefficient of determination (R^2). Among all models Normalized Difference Turbidity Index (NDTI) [17], was found to exhibits a strong relation with *in situ* measure turbidity.

$$NDTI = \frac{R_{Red}(B3) - R_{Green}(B2)}{R_{Red}(B3) + R_{Green}(B2)} \quad (3)$$

where $R_{Red(B3)}$ is reflectance in Red band, $R_{Green(B2)}$ is reflectance in Green band.

A flow chart of the methodology is shown in Figure 2. Pre-processing of the Level 1 GTD RS2 and R2A LISS-III data is required for conversion of the Digital Number (DN) values to Top of Atmosphere) TOA) reflectance data. The derived radiance values were converted to TOA reflectance using solar exo-atmospheric irradiance (E_o) values of RS2 LISS- III sensor [22]. The removal of atmospheric additive constant haze removal is done using simple dark object subtraction (SDOS) for multispectral image [9].

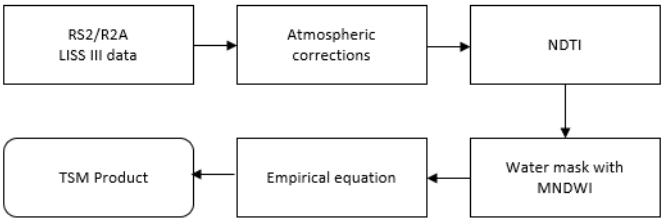

Figure 2. Systematic flow chart of processing RS2 and R2A LISS-III images

IV. RESULTS AND DISCUSSION

The correlation analysis showed that there was a significant co-relation between simulated RS2 and R2A LISS-III derived NDTI and insitu measured turbidity. Both the IRS-RS2 and R2A LISS-III derived algorithm shows a strong coefficient of determination (R^2 = 0.97) with the *in situ* turbidity measurements, which is also shown in Figure 3 (A and B). For other combinations like reflectance in Green, Red and NIR bands, the observed coefficient of determination was found to be 0.57, 0.90 and 0.74 respectively. Although the Red band also provide a good corelation but NDTI based algorithm was found to be performimg better for different seasons.

The derived algorithm are represented as

$$\text{Turbidity}_{\text{(IRS-RS2) LISS-III}}\ (\text{NTU}) = 106.17x^2 + 91.46x + 21.83 \quad (4)$$

$$\text{Turbidity}_{\text{(IRS-R2A) LISS-III}}\ (\text{NTU}) = 107.16x^2 + 92.41x + 22.05 \quad (5)$$

where the x is NDTI derived values.

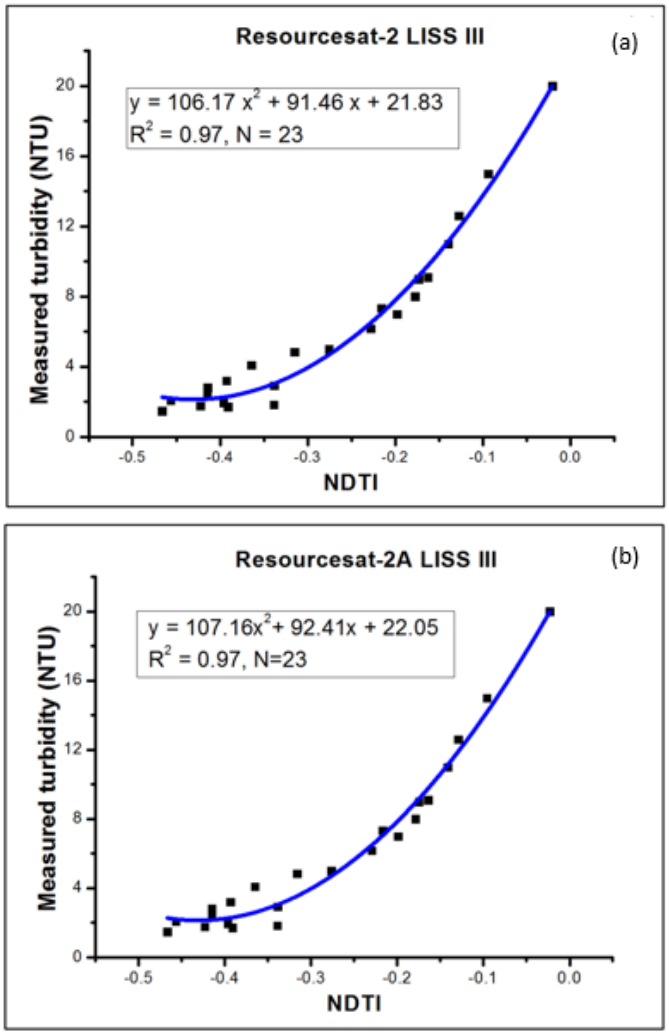

Figure 3. Scatter plots of turbidity algorithm calibration (A & B) between *in situ* measured turbidity measurement data and simulated RS2 and R2A LISS-IIIderived NDTI.

Figure 4 shows the turbidity variation over the Ukai reservoir derived using new turbidity algorithm (equations 4 and 5) for 19 cloud free IRS-R2A (4) and IRS-RS2 (15) LISS-III images, from 2012 to 2018 in pre monsoon season (March, April and May months). Reservoir surface area was estimated using MNDWI. In the month of March, the reservoir surface area was ranges from 272.14 to 429.60 km ^{2}, for the same month turbidity ranges from 2.31 to 30.56 NTU. In April, the reservoir surface area was ranges from 225.91 to 397.96 km ^{2}, for the same month turbidity ranges are from 3.55 to 31.65 NTU. In the month of May, reservoir surface area varied from 192.47 to 310.46 km ^{2}, for the same month turbidity ranges from 2.97 to 32.63 NTU. More details about the surface area and turbidity variation are provided in the Table 3.

Table 3. Derived turbidity and Surface area of ukai reservoir during 2012-2018 pre monsoon season

Date	Surface area (km^2)	Turbidity (NTU)			
		Minimum	Maximum	Mean	S.D
2012-03-02	392.68	2.97	25.73	5.01	4.93
2012-03-26	362.99	3.11	24.73	4.85	4.57
2013-03-21	371.40	3.37	29.50	6.94	7.27
2013-04-14	339.60	5.13	30.43	9.88	7.13
2013-05-08	305.08	6.85	31.25	8.03	4.65
2014-03-16	429.60	3.00	19.83	4.37	3.17
2014-04-09	397.96	3.55	31.65	7.81	7.44
2015-03-11	343.51	2.97	30.56	8.15	7.47
2015-04-28	263.32	5.36	30.56	8.03	7.12
2015-05-22	232.44	6.96	31.56	8.66	7.96
2016-03-05	315.54	2.86	29.80	6.58	6.92
2016-04-22	225.91	5.69	31.62	8.26	7.03
2016-05-16	192.47	5.02	32.63	7.14	5.69
2017-03-12	416.09	3.41	25.80	5.22	4.32
2017-04-05	382.01	4.45	26.31	7.89	6.06
2017-05-11	310.46	7.06	30.09	8.29	6.89
2018-03-31*	272.14	2.31	22.95	5.57	5.66
2018-04-24	227.62	5.79	23.77	8.65	5.57
2018-05-06	208.02	2.97	31.26	7.96	5.69

The lowest turbidity value (2.31 NTU) was observed on 31st March 2018 while the highest value (32.63 NTU) was observed on 16th May 2016. The highest value was more than fourteen times greater than the lowest value, which represents high turbidity variation in Ukai reservoir.

The lowest surface area (192.47 km^2) of reservoir was also observed on the same day of highest turbdity, it indicates that the turbidity is inversely realated to the surface area of water body in our analysis, but we can't make a conclustion each and every time the relation will work, number of factors will infulence water turbidity. The *in situ* measured turbidity over the reservoir was ranges between 1.47 - 20 NTU, with mean value 6.14 NTU and Standard deviation (S.D.) 4.75 NTU.

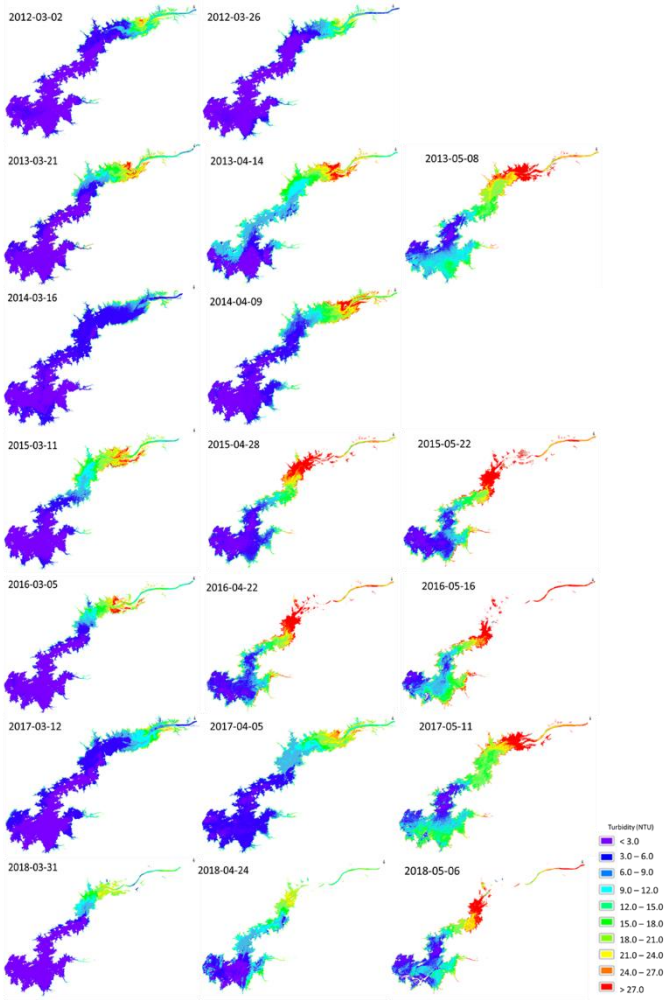

Figure 4. Derived turbidity (NTU) distribution maps in the Ukai Reservoir from 2012 to 2018 pre monsoon season

For further understanding the turbidity spatial variations within the reservoir, we have divided the reservoir area into 3 parts, i.e. Down (A), Middle (B) and Up streams (C) (as marked in Figure 1). The mean turbidity in down stream was always lower than the middle and up streams during 2012-2018. Down stream lowest and highest mean turbidity was 2.31 NTU on 31st March 2018 and 8.02 NTU on 06th May 2018 respectively with S.D. of 1.78 NTU. Up stream consistantely shows highest urbidity values than the other portion of reservoir, with a minimum mean turbidity 6.81 NTU on 16th March 2014 and maximum mean turbidity 22.80 NTU on 14th April 2013 with S.D. 4.47 NTU.

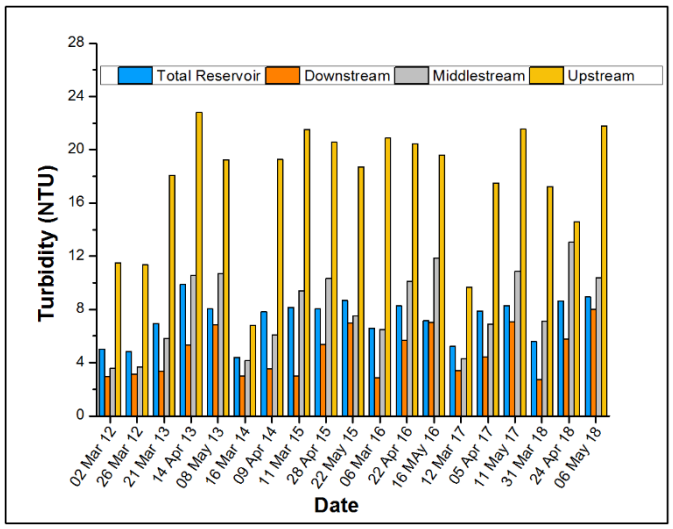

Figure 5. Derived mean Turbidity for whole Ukai reservoir and three sub regions Down (A), Middle (B) and Up Streams (C)

Seven years turbidity patterns in pre monsoon season were quantified with satellite data sets of RS2 and R2A LISS-III, however uncertainities in quantification of turbidity was still not known. Ideally, Ukai reservoir may be evaluated based on more number of samples and low temporal resolution data than RS2 and R2A LISS-III, for better understanding of seasonal and interannual turbidity patterns. Although there are other satellite data sets are availible like MODIS insturments etc, with the low temporal resolution, but they have a comparitively poor spatial resolution for such studies. Both RS2 and R2A LISS-III sensors are having similar spatial and spectral resolutions, so it provides a good opportunity to observe long-term variations with nearly same consistency.

V. CONCLUSIONS

Sensor specific, Green and Red band based algorithm was developed for assessment of turbidity in NTU units for Ukai reservoir. The developed algorithm was used to derive 2012-2018 pre monsoon turbidity maps, *in situ* measured turbidity rages are 1.47 to 20 NTU, with a mean of 6.14 and standard deviation of 4.75 NTU. As per our knowledge, we attempt to develop algorithm for turbidity over Ukai reservoir using RS2 and R2A LISS-III data. Derived algorithm shows a strong coefficient of determination (R^2 = 0.97) with the *in situ* turbidity measurements, derived turbidity ranges are the lowest turbidity value was 2.31 NTU on 31st March 2018 and the highest was 32.63 NTU on 16th May 2016. Maximum turbidity was fourteen times greater than the lowest value, which shows that high variation in turbidity in the Ukai reservoir. Both down and middle stream mean turbidity ranges are below the 20 NTU which was measured in field observations, out of 19 images except seven images in the up stream mean turbidity was more than the 20 NTU.

In brief, this study provides (1) a new algorithm for assessment of turbidity over Ukai reservoir during 2012-2018 (7 years) pre monsoon season and (2) An empirical method that applied a thorough analysis to derive turbidity variation between RS2 and R2A LISS-III sensors. Neverthless, some uncertainties will always remain with the empirical algorithms; in the future study should be conducted to incorporate factors such as particle size, shape, colour and mineral type as well as organic substance and chlorophyll that may affect the optical properties of turbid waters. Results obtained through this study could serve as a basic foundation for the assessment of turbidity and remaining water quality parameters in Ukai reservoir, and it also be used in various numerical modles to help characterize the trophic state of an inland aquatic ecosystem.

VI. ACKNOWLEDGMENTS

The authors are thankful to Shri. Nilesh M Desai, Director, Space Applications Centre (SAC), Indian Space Research Organisation (ISRO) and Dr. Ish Mohan Bahuguna, Deputy Director, Earth, Ocean, Atmosphere and Planetary Sciences and Applications Area (EPSA), SAC for their overall support. The work was carried out under GISAT: Science and Application Project. Authors are also thankful to Executive Engineer Ukai Division No 1, Ukai and District Forest Officer Vyara, District –Tapi for helping in carrying out the water quality measurements over Ukai reservoir.

VII. REFERENCES

[1]. Analytical Spectral Devices, Inc. (ASD). (2006). FieldSpec® 3 User Manual.

[2]. Bastamante, J., Pacios, F., Diaz-Delgado, R., & Aragonés, D. (2009). Predictive models of turbidity and water depth in the Doñana marshes using LANDSAT TM and ETM+ images. Journal of Environment management, 90, 2219-2225.

[3]. Bilge, F., Yazici, B., Dogeroglu, T., & Ayday, C. (2003). Statistical evaluation of remotely sensed data for water quality monitoring. International Journal of Remote Sensing, 24,5317-5326.

[4]. Bowers, D. G., Braithwaite, K. M., Nimmo-Smith, W. M., & Graham, G. W. (2009). Light scattering by particles suspended in the sea: The role of particle size and density. Cont. Shelf Res., 29, 1748-1755.

[5]. Buttner, G., Korndi, M., Gyomorei, A., Kote, Z., & Szabo, G. (1987). Satellite Remote Sensing of Inland Water: Lake Balaton and Reservoir Kiskore. ActaAstronautica, (6/7), 305-311.

[6]. Campbell, G., Phinn, S. R., Dekker, A. G., & Brando, V. E. (2011). Remote sensing of water

Quality in an Australian Tropical Freshwater Impoundment using Matrix Inversion and MERIS Images. Remote sensing of Environment, 115, 2402-2414.

[7]. Carlson, R. E. (1977). A Tropic State Index for Lakes. Limnology and Oceanography, 22, 361-369.

[8]. Cerco, C. F., Kim, S. C., & Noel, M. R. (2013). Management modelling of suspended solids in the Chesapeake Bay, USA.Estura. Coast.Shelf Sci., 116, 87-98.

[9]. Chavez, P. S., & Jr. (1988). An Improved Dark-Object Subtration Technique for Atmosphere Scattering Correction of Multispectrl Data . Remote Sensing of Environment , 24:459-479.

[10]. Choubey, V. K. (1992). Correlation of tubidity with indian Remote Sensing Satellite-1A data. Hydrological Sciences, 37(2), 129-140.

[11]. Dihkan, M., Karsil, F., & Guneroglu, A. (2011). Mapping total suspended matter concentrations in the Black sea using Landsat TM multispectral imagery. Fresenius Environ. Bull., 20, 262-269.

[12]. Gholizadeh, M. H., Melesse, A. M., & Reddi, L. (2016). A comprehensive review on water quality parameters estimation using remote sensing techniques. Sensors, 16,1298.

[13]. Goodin, D. G., Harrington, J. A., Jr, Druane Nellis, M., & Rundquist, D. C. (1996). Mapping reservoir turbidity patterns using SPOT-HRV data. Geocarto International, 11 (4), 71-78.

[14]. Grove, M. K., Bilotta, G. S., Woockman, R. R., & Schwartz, J. S. (2015). Suspended sediment regimes in contrasting reference-condition freshwater ecosystems: Implications for water quality guidelines and management. Sci. Total Environ., 502, 481-492.

[15]. Khorram, S., Cheshire, H., Geraci, A., & Rosa, G. (1991). Water Quality Mapping of Augusta Bay, Italy from Landsat TM Data. International Journal of Remote Sensing, 12(4), 803-808.

[16]. Koponen, S. J., Pulliainen, K. K., & Hallikainen, M. (2002). Lake Water Quality Classification with airborne Hyperspectral Spectromenter and Simulated MERIS Data. Remote sensing of Environment, 79, 51-59.

[17]. Lacaux, J. P., Tourre, Y. M., Vignolles, C., Ndione, J. A., & Lafaye, M. (2007). Classification of ponds from high-spatial resolution remote sensing: Application to Rift vally Fever epidermics in Senegal. Remote Sens. Environment, 106,66-74.

[18]. Liversedge, L. (2007). Turbidity mapping and prediction in ice marginal lakes at the Bering Glacier System, Alaska. (M.S. thesis). University of Michigan, School of natural Resources and Environment, (50 pp.).

[19]. Massicotte, P., Gratton, D., Frenette, J. J., & Assani, A. A. (2013). Spatial and temporal evolution of the St. Lawrence River spetral profile: A 25 year case study using landsat 5 and 7 imagery. Remote Sens. Environ., 136, 433-441.

[20]. Morel, A. (1988). Optical modelling of the upper ocean in relation to its biogenous matter content (case I waters). J.Geophys. Res. Oceans, 93, 1074-1086.

[21]. Morel, A., & Mueller, J. L. (n.d.). Normalized water-leaving radiance and remote sensing reflectance: Bidirectional reflectance and other factors. Retrieved from Available online:http://ntrs.nasa.gov/archive/nasa/casi.ntrs.nasa.gov/20020044099.pdf

[22]. Nechad, B., Ruddick, K. G., & Park, Y. (2010). Calibartion and validation of a generic multisensor algorithm for mapping of total suspended matter in turbid waters. Remote Sens. Environ., 114, 854-866.

[23]. Pandya, M. R., Singh, R. P., Murali, K. R., Babu, P. N., Kirankumar, A. S., & Dadhwal, V. K. (2002). Bandpass solar exoatmospheric irradiance and Rayleigh optical thickness for IRS satellite sensors onboard IRS-1A, 1B, 1C, 1D and P4. IEEE Transaction on Geoscience and Remote Sensing, 714-718.

[24]. Petus, C., Chust, G., Gohin, F., Doxaran, D., Froidefond, J. -M., & Sagarminaga, Y. (2010). Estimating turbidity and total suspended matter in the Adour River plume (South Bay of Biscay) Using MODIS 250-m imagery. Continental Shelf Research, 30, 379-392.

[25]. Pompapathi, V., Shard Chander, Ashwin Gujrati, Solanki, H. A., & Singh, R. P. (2021). Monitoring of Turbidity Variation in the Ukai Reservoir, Gujarat, INDIA, during 1993-2018 using Landsat Series of Dataset. International Journal of Scientific Research in Science and Technology (IJSRST), 8(6), 236-251.

[26]. Pulliainen, J., Kallio, K., Eloheimo, K., Koponen, S., Servomaa, H., Hannonen, T., . . . Hallikainen, M. (2001). A Semi Operative Approach to Lake Water Quality Retrieval from Remote Sensing Data. The Science of the Total Environment, 268, 79-93.

[27]. Skarbovik, E., Stalnacke, P., Bogen, J., & Bones, T. E. (2012). Impact of sampling frequency on mean concentrations and estimaed loads of suspended sediment in a Norwegian river. implications for water management.Sci. Total Environ., 462-471.

[28]. Tang, J. W., Tian, G. L., Wang, X. Y., Wang, X. M., & Song, Q. J. (2004). The methods of water spectra measurement and analysis I: Above-water method. J.Remote Sens. Beijing, 8,37-44.

[29]. Xu, H. (2006). Modification of normalised difference water index (NDWI) to enhance open water features in remotely sensed imagery. International Journal of Remote Sensing, 3025-3033.

[30]. Zhang, M. W., Dong, Q., Cui, T. W., Xue, C. J., & Zhang , S. L. (2014). Suspended sediment monitoring and Assessment for yellow River eastury from landsat TM and ETM plus imagery. . Remote Sens. Environ., 146, 136-147.

[31]. Zhang, Y., Pulliainen, J., Koponen, S., & Hallikainen, M. (2002). A semi-Empirical Algorithm of water Transparency at the Green Wavelength Band of Optical Remote Sensing. Progress in Electromagnetic Research, 37, 191-203.

[32]. Zibordi, G., Voss, K. J., Johnson, B. C., & Mueller, J. L. (2019). IOCCG Ocean Optics and Biogeochemistry Protocols for Satellite Ocean Colour Sensor Validation, volume 3.0. IOCCG, Dartmouth, NS, Canada. doi:http://dx.doi.org/10.25607/OBP-691

Cite this article as :

V. Pomp